Received: 22 April 2019 | Revised: 5 March 2020 | Accepted: 9 March 2020

DOI: 10.1002/jbm.a.36932

ORIGINAL ARTICLE

Society For Biomaterials | WILEY

Bioreactor cultivation condition for engineered bone tissue: Effect of various bioreactor designs on extra cellular matrix synthesis

Hanieh Nokhbatolfoghahaei[1] | Mahboubeh Bohlouli[2,3] | Zahrasadat Paknejad[4] | Maryam R. Rad[1] | Leila M. Amirabad[5] | Nasim Salehi-Nik[6] | Mohammad M. Khani[3] | Shayan Shahriari[7] | Nasser Nadjmi[8] | Adel Ebrahimpour[9] | Arash Khojasteh[1,3]

[1]Dental Research Center, Research Institute of Dental Sciences, Shahid Beheshti University of Medical Sciences, Tehran, Iran

[2]Student Research Committee, Medical Nanotechnology and Tissue Engineering Research Center, Shahid Beheshti University of Medical Sciences, Tehran, Iran

[3]Department of Tissue Engineering and Applied Cell Sciences, School of Advanced Technologies in Medicine, Shahid Beheshti University of Medical Sciences, Tehran, Iran

[4]Medical Nanotechnology and Tissue Engineering Research Center, Shahid Beheshti University of Medical Sciences, Tehran, Iran

[5]School of Dentistry, Marquette University, Milwaukee, Wisconsin

[6]Department of Biomechanical Engineering, Faulty of Engineering Technology, University of Twente, Enschede, The Netherlands

[7]Department of Biomedical Engineering, Science and Research Branch, Islamic Azad University, Tehran, Iran

[8]The Team for Cleft and Craniofacial Anomalies, Oral and Maxillofacial Surgery, University of Antwerp, Antwerp, Belgium

[9]Department of Orthopedics, Shahid Beheshti University of Medical Sciences, Tehran, Iran

Correspondence
Arash Khojasteh, Department of Tissue Engineering and Applied Cell Sciences, School of Advanced Technologies in Medicine, Shahid Beheshti University of Medical Sciences, Tehran, Iran.
Email: arashkhojasteh@gmail.com

Funding information
Iran Ministry of Health and Medical Education, Grant/Award Number: 700/1702

Abstract

Dynamic-based systems are bio-designed in order to mimic the micro-environments of the bone tissue. There is limited direct comparison between perfusion and perfusion-rotation forces in designing a bioreactor. Hence, in current study, we aimed to compare given bioreactors for bone regeneration. Two types of bioreactors including rotating & perfusion and perfusion bioreactors were designed. Mesenchymal stem cells derived from buccal fat pad were loaded on a gelatin/β-Tricalcium phosphate scaffold. Cell-scaffold constructs were subjected to different treatment condition and place in either of the bioreactors. Effect of different dynamic conditions on cellular behavior including cell proliferation, cell adhesion, and osteogenic differentiation were assessed. Osteogenic assessment of scaffolds after 24 days revealed that rotating & perfusion bioreactor led to significantly higher expression of OCN and RUNX2 genes and also greater amount of ALP and collagen I protein production compared to static groups and perfusion bioreactor. Observation of cellular sheets which filled the scaffold porosities in SEM images, approved the better cell responses to rotating & perfusion forces of the bioreactor. The outcomes demonstrated that rotating & perfusion bioreactor action on bone regeneration is much preferable than perfusion bioreactor. Therefore, it seems that exertion of multi-stimuli is more effective for bone engineering.

KEYWORDS

bone regeneration, buccal fat pad-derived stem cells, perfusion & rotating bioreactor, perfusion bioreactors, β-TCP

1 | INTRODUCTION

Positive impact of dynamicity in biological systems for functional bone engineering has gain scientific consensus and methodical evidences. Dynamic-based systems are bio-designed in order to mimic the micro and macro-environments of the bone tissues and to match their mechanical and physiological characteristics (Qian, Yuan, Zhimin, & Anchun, 2013). The primary function of skeleton is to bear the body loads with respect to individual weight and physical activities, so a bone tissue is under constant mechanical stimulations. This dynamic bone loading causes extra-cellular matrix (ECM) deformation and lacuno-canalicular fluid flow (Lim et al., 2012; Liu et al., 2014; McCoy & O'Brien, 2010). The resultant hydrostatic pressure is directly sensed by bony cells, highly mechanosensitive compartments of bone tissue (Rauh, Milan, Guenther, & Stiehler, 2011). The flow-induced interstitial shear stress has been ascribed as an active force for directing cellular differentiation (McCoy & O'Brien, 2010) and subsequent bone remodeling by activation of extracellular ERK1/2, Wnt, bone morphogenic protein (BMP) signaling pathways (Charoenpanich et al., 2011; Ho et al., 2008; Holguin, Brodt, & Silva, 2016; Hou, Zhu, Zhou, Zhang, & Yu, 2011; Ikegame et al., 2016; Li et al., 2015; Wang et al., 2015; Wu, Zhang, Zhang, Fang, & Jiang, 2012; Zhang, Wu, Jiang, Jiang, & Fang, 2012). Therefore, mechanical encounter is of great importance in the processing of bone regeneration in vivo. However, the majority of in vitro investigations are conducted on static cultural settings which neglect the pivotal role of mechanical stimulations in bone tissue engineering. The drawbacks of static culture environment including limited expression of osteogenic markers and lower differentiation of stem cells, as well as a restricted diffusive transport of nutrients to the scaffold core (Katayama, Arano, Sato, Ikada, & Yoshinari, 2012; Nokhbatolfoghahaei, Rad, Khani, Nadjmi, & Khojasteh, 2017; Yeatts et al., 2013) have driven researches toward the incorporation of mechanical stimuli through streaming the culture medium in the scaffold using bioreactors (Nokhbatolfoghahaei et al., 2017).

In this regard, a number of bioreactor systems have been designed to promote physiological relevance for the bone tissues. The application of hydrodynamic shear stress by circulation of medium fluid within the system is one of the most straight-forward and commonly used bioreactor designs. Spinner flasks, rotating wall vessel, and perfusion bioreactors are categorized as shear-loading devices. Although the spinner flask apparatus alleviates the external nutrient transfer problems of scaffolds, but the internal constraints remains challenging. Besides, the turbulent environment generated by stirring medium can potentially dissociate the attached cells (David et al., 2011). Rotating wall vessel bioreactors leads to small shear stresses and high rates of nutrient transfer (David et al., 2011). In the preliminary models of rotating wall vessel bioreactors, cell-loaded constructs are freely floated in the fluid and are negatively subjected to collision with the bioreactor wall which can damage the scaffold and detach the adhered cells. So, a different design of rotating wall vessel bioreactor invented in form of rotating bed bioreactor in which the seeded scaffolds are tightly held on a rotating axis (Rauh et al., 2011). Although, rotating systems provide higher cell proliferation and differentiation in comparison with spinner flask culturing, but similarly medium infiltration is confined to the outer layers of scaffolds (Rauh et al., 2011). Due to the limitation of mass transport through the organoid construct, perfusion-based bioreactors were introduced. This system generates a laminar fluid flow through the chamber by piping the medium with a peristaltic pump and demonstrate an affective set to supply uniform medium delivery into the scaffold pores (Vetsch, Müller, & Hofmann, 2015).

Among various types of shear-loading bioreactor designs, the perfusion bioreactors are considered the most efficient devices for bone tissue engineering. Beside, according to the effort which systematically reviewed the studies on the application of bioreactors for functionality evaluation of bone, approximately 73% of researchers employ perfusion bioreactors alone, potentially due to its exclusive capability in medium diffusion inside the scaffolds (Nokhbatolfoghahaei et al., 2017). It has been evidenced that bioreactors utilizing a combination of forces, such rotation plus perfusion, significantly enhanced cell growth and higher activity of alkaline phosphatase enzyme, a presenter of osteogenic differentiation (Bölgen et al., 2008; Jagodzinski et al., 2008). Hence, fabrication a device using combined practical approaches is an attractive strategy. However, there is limited direct comparison between perfusion and perfusion-rotation forces in designing a bioreactor-based bone tissue engineering.

Given that, in this study, we intended to compare these two type of designs in cellular behaviors of mesenchymal stem cells (MSCs) loaded on a 3D β-Tricalcium phosphate (β-TCP) scaffold which is reinforced with gelatin, due to its appropriate characteristics. MSCs from buccal fat pad (BFPdSCs) were the stem cell of choice for this assessment. BFP can be harvested easily with minimal discomfort and complications for patient. Furthermore, stem cells isolated from this tissue have high proliferation rate and osteogenic differentiation capability in vitro and in vivo (Rezai Rad et al., 2017; Salehi-Nik et al., 2017).

2 | MATERIALS & METHODS

2.1 | Materials

Collagenase type I, β-Glycerol phosphate disodium salt pentahydrate, Acid Ascorbic, Dexamethasone, Alizarin Red (A3757), CellLyticTM tissue lysis buffer (C3228), Alkaline Phosphatase yellow liquid substrate (P7998), Xylol, Paraffin, 4′,6-diamidino-2-phenylindole (DAPI), and phosphate buffer saline (PBS) were purchased Sigma-Aldrich, St. Louis, MO. 0.25% trypsin/Ethylenediaminetetraacetic acid (EDTA), Dulbecco's Modified Eagle's Medium (DMEM)-high glucose, Fetal Bovine Serum (FBS), Penicillin, and Streptomycin (pen/strep) antibiotic, cDNA synthesis kit DMEM-low glucose were purchased Thermo Fisher Scientific, Waltham, MA. Also, Paraformaldehyde, Ethanol, Glutaraldehyde from Merck, Kenilworth, NJ and anti-Collagen I (abcam 34710), Alkaline Phosphatase (abcam 65834), and Secondary antibody were purchased ABCAM, Cambridge, UK. Anti-CD44, Anti-CD105, Anti-CD34 were from EXBio, Vestec, Czech Republic. Anti-CD73, Anti-CD45, and also hematoxylin and eosin (H&E) (E12169) were

purchased e Biosciences, San Diego, CA. RNX-plus reagent and Green Master Mix kit were purchased from Sinaclon, Tehran, Iran and Ampliqon, Odense M, Denmark, respectively.

2.2 | System design

Two bioreactors including perfusion (P) and rotating & perfusion (R&P) bioreactors were designed. The R&P bioreactor (Figure 1a), consists of five main parts: (a) A glass-made chamber with external and internal diameters of 18.5, 15 mm, respectively, (b) The perfusion system consists of a peristaltic pump (505S, Watson-Marlow, Falmouth, Cornwall, UK) that transfers medium from reservoir to chamber with flow rate of 1–2 ml/min through an autoclavable silicone tube (Cole Parmer, Vernon Hills, IL), (c) The rotational system induced by a stepper motor with 1 rpm in order to avoid gravitation effect on the cell-scaffold construct during cultivation, (d) Glass-made medium reservoir with silicone cap that has three holes for connection of inlet and outlet tubes, and an air ventilation (0.2 μm filter, membrane solutions, TX), and (e) Electronic circuit and control panel responsible for rotational adjustment.

The Perfusion bioreactor (Figure 1b), designed according to the Grayson et al. model (Grayson et al., 2008), with minor modifications. The perfusion bioreactor consists of two main parts: (a) perfusion system with a peristaltic pump (505S, Watson-Marlow, Falmouth, Cornwall, UK) that circulate culture medium with flow rate of 1–2 ml/min in each wells through autoclavable silicone tube (Cole Parmer, Vernon Hills, IL), (b) The chamber made from poly methyl methacrylate and silicone sheets between the poly methyl methacrylate layers for sealing. The bioreactor chamber also serves as a reservoir. An air ventilator (0.2 μm filter, membrane solutions) was installed on bioreactor cap to exchange oxygen.

2.3 | β-TCP scaffolds coated with gelatin (gTCP) fabrication

A comprehensive description to the fabrication of gTCP scaffolds has been explained in our previous study (Bastami et al., 2017). The total porosity was 70.6 ± 1.8% and the mean pore size was 191.9 ± 74.6 μm (min: 72.8 μm, max: 334.8 μm) (Supporting Information S1) (Figure 1c-f).

2.4 | Cell isolation and culture

2.4.1 | Cell isolation

Buccal fat pad (BFP) tissue was collected from young and healthy volunteer donor cell isolation was immediately performed using enzymatic digestion protocol, explained in the previous study (Rezai Rad et al., 2017). Briefly, the tissue was washed with PBS, digested in a solution of 3 mg/ml collagenase type I and shook for 30 min at 37°C.

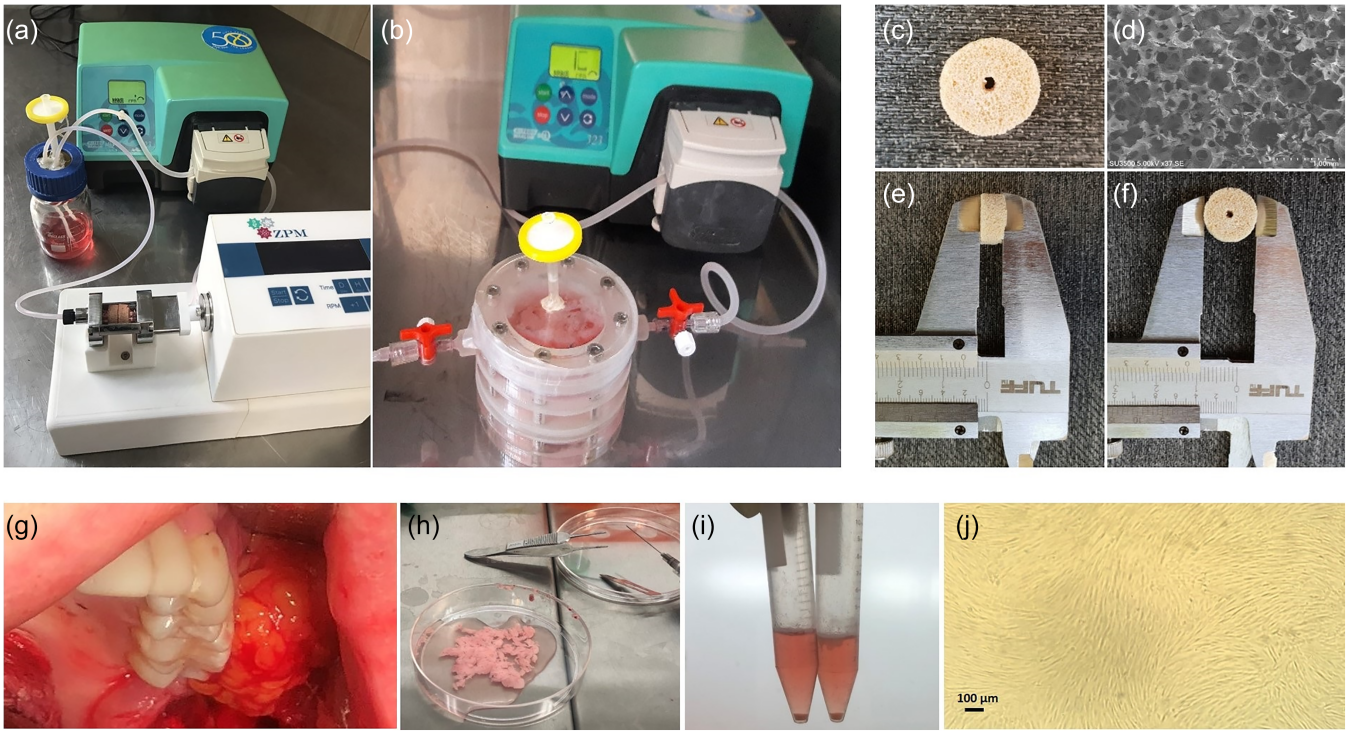

FIGURE 1 (a) Bioreactor R&P, (b) Bioreactor P, (c) Photography image of 3D gelatin coated β-tricalcium phosphate scaffolds. (d) SEM image of scaffold represented the presence of interconnected and micro- and macro-sized pores, (e,f) Measurement of scaffold thickness and diameter using calipers (thickness = 5 ± 0.5, diameter = 12 ± 0.5 mm). (g) Cell isolation was carried out from buccal fat pad (h,i) The tissue was minced into small pieces, dissociated with collagenase and centrifuged to obtain cellular pellet in the Falcone. (j) The isolated cells were transferred into culture flasks containing standard medium

(Figure 1g-j). After centrifugation, the BFPdSCs were washed with PBS and cultured in the standard medium containing DMEM-high Glucose, 15% FBS, 10× pen/strep until three passage.

2.4.2 | Cell characterization

In this study, flow cytometry and Alizarin red staining have been used to confirm the stemness and representing MSCs phenotype of isolated BFPdSCs at three passage.

Flowcytometry

BFPdSCs were incubated with fluorescein isothiocyanate and phycoerythrin conjugated antibody for 30 min at 4°C in a dark room. Then, cells were washed and analyzed using Attune® Acoustic Focusing Cytometer (Applied Biosystems, Foster City, CA), and the FLOWJO 7.6.1 software (TreeStar, San Carlos, CA). Fluorescein isothiocyanate-conjugated antibodies were anti-CD90, anti-CD73, anti-CD44, and anti-CD45. Phycoerythrin-conjugated antibodies were anti-CD105 and anti-CD34.

Alizarin red staining

BFPdSCs were cultured in osteogenic medium for 14 days, then extracellular calcium deposition was detected by Alizarin red staining (Supporting Information S2).

2.5 | Cell seeding and study design

After sterilization of scaffolds (Supporting Information S3), The BFPdSCs were seeded on both sides of scaffolds at a density of 1×10^6 viable cell/scaffold. After 2 hr incubation, standard medium was added to scaffolds. In order to determine the effect of mechanical stimuli on cellular behaviors, following treatment groups were considered: (a) Negative control group (Neg Control) contains cell/scaffolds incubated in standard medium for 24 days, (b) Positive Control (Pos Control) includes cell/scaffolds which are incubated in standard medium for 3 days and osteogenic medium for 21 day, (c) Bioreactor R&P group consist of cell/scaffolds which incubated in standard medium for 3 days, then 5 days in osteogenic medium in static condition, followed by 16 days in osteogenic medium in Bioreactor R&P, (d) Bioreactor P group includes scaffolds which are cultured in similar condition as Bioreactor R&P group (Figure 2). Two bioreactors were sterilized as follow. The perfusion bioreactor chamber was sterilized using UV light and other components of this bioreactor and rotating/perfusion bioreactor were autoclaved for 20 min at 121°C and 15 pounds pressure.

2.6 | Biological assessments

2.6.1 | Glucose uptake and consumption

Metabolic activity of BFPdSCs on various dynamic cultures was monitored by measuring glucose concentration from culture medium after initiation of osteogenic differentiation. This concentration was analyzed using Roche Hitachi 912 chemistry analyzer (Roche diagnostic, Indianapolis, IN). The following formula was used to measure the amount of glucose consumed by the cells:

$$\text{Glucose consumption} = \text{Conc.Glu}\,t_0 - \text{Conc.Glu}\,t_1$$

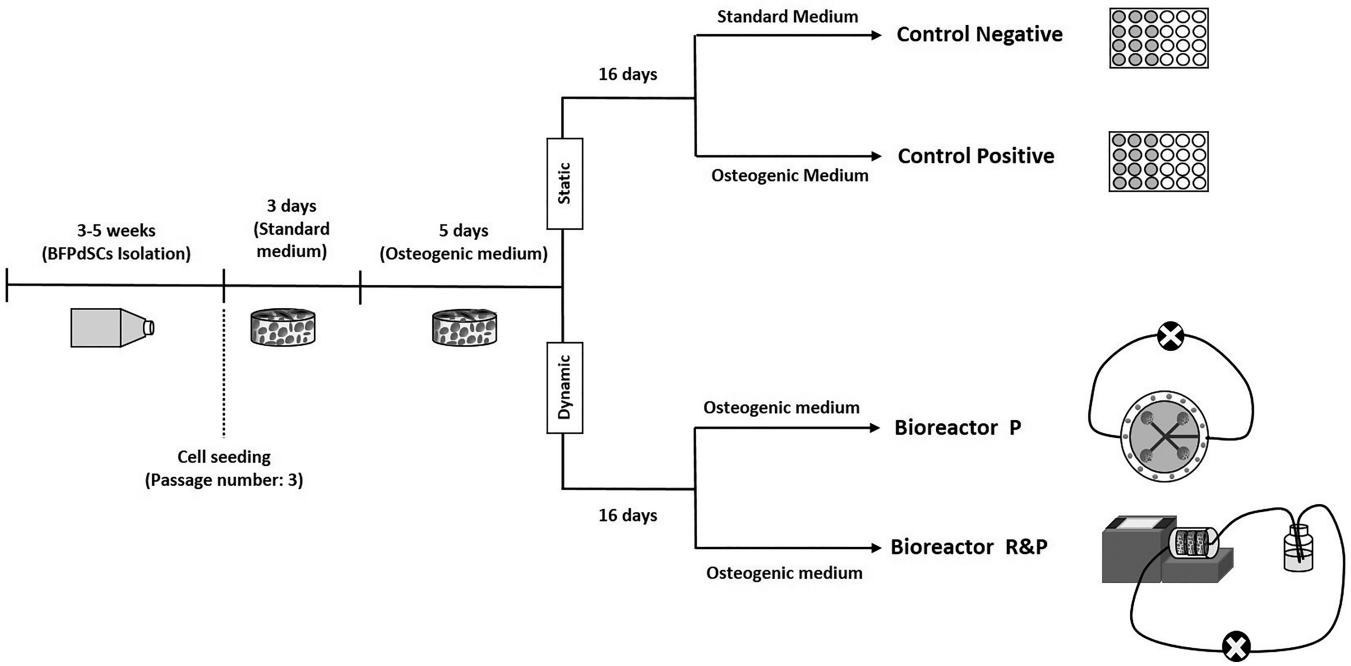

FIGURE 2 Study design diagram

where t_0 = initial time point, t_1 = test time point, Conc = concentration, and Glu = glucose.

2.6.2 | Alkaline phosphatase (ALP) activity assay

ALP activity of cells was evaluated by the specific conversion of P-nitrophenyl phosphate to P-nitrophenol after 24 days. The absorbance of formed P-nitrophenol was read at 405 nm by ELIZA reader (BioTek, Winooski, VT) (Supporting Information S4).

2.6.3 | Scanning electron microscopy (SEM) analysis

Initially, the cell-scaffold constructs were fixed and dehydrated by 2.5% glutaraldehyde and a graded series of ethanol, respectively. Then, the scaffolds were mounted on stubs and with sputtered gold/palladium coated. Then imaged were captured using SEM device (Akishima Tokyo, Japan) (Supporting Information S5).

2.6.4 | Histology and immunohistochemistry (IHC) analysis

For IHC staining, sample sections (Supporting Information S6) were incubated with primary antibodies against Collagen I (abcam 34710) and Alkaline Phosphatase (abcam 65834), followed by secondary antibody. Then, nuclei were counterstained with DAPI. Semi-quantitative analysis was performed by a computerized video camera-based image analysis system under fluorescence microscope (Nikon, Minato, Tokyo, Japan).

2.6.5 | Real time quantitative PCR

The osteogenic differentiation capability of cell-scaffold constructs were assessed by evolution of expression osteogenic markers, such as β-actin, Runt-related transcription factor 2 (RUNX2), and osteocalcin (OCN) using Real Time quantitative PCR (Supporting Information S7) (Table 1).

2.7 | Statistical analysis

All the quantitative results were obtained from triplicate samples. These results are expressed as mean ± *SD*. One-way analysis of variance (ANOVA) and independent sample T-test were performed by SPSS software for windows (version 15.0; SPSS, Chicago, IL). The difference were considered with a confidence interval 95% (α = .05) for all analyses. *SD* error bars are showed on each figure.

TABLE 1 Osteogenic markers' primer

Gene name	Direction	Sequence 5′ to 3′
Runx2-F	Forward	GAACCCAGAAGGCACAGACA
Runx2-R	Reverse	ACTTGGTGCAGAGTTCAGGG
OCN-F	Forward	CACTCCTCGCCCTATTGGC
OCN-R	Reverse	CCCTCCTGCTTGGACACAAAG
B-Actin-F	Forward	ATGCCTGCCGTGTGAAC
B-Actin-R	Reverse	ATCTTCAAACCTCCATGATG

3 | RESULTS

3.1 | Characterization of human BFPdSCs

Fibroblast-like cells isolated from BFP was evaluated for expression of stemness markers and differentiation potential at three passage. The flow cytometry analysis showed that these cells expressed CD90 (87.5%), CD73 (82.9%), CD105 (70.5%), CD44 (74.5%), CD34 (2.78%), and CD45 (1.43%). Data evidenced that isolated cells had high population with MSC phenotypes (Figure 3a).

Also, to confirm the osteogenic capability of cells, BFPdSCs were cultured in an osteogenic and standard culture medium prior to staining with Alizarin Red for 14 days. Extracellular calcium deposition was significantly higher in osteogenic medium-incubated samples compared to standard medium (Figure 3b).

3.2 | Effect of dynamic bioreactors on BFPdSCs

3.2.1 | Metabolic activity

Glucose consumption was measured as a marker of BFPdSCs metabolic activity on gTCP scaffold. D-glucose consumption rate was approximately similar among two bioreactors after 24 days. These results showed that D-glucose consumption rates increased steadily days after induction of osteogenic differentiation until 14 and decreased after this time point (Figure 3c).

3.2.2 | Cell adhesion and colonization

The adhesion of the BFPdSCs and ECM production on the gTCP scaffolds in static and dynamic condition was evaluated by Scanning Electron Microscopy (SEM) micrographs. As it shown in Figure 4, during 24 days of cultivation, except for control negative group, cells were infiltrated through the pore of scaffold in all groups. Furthermore, it was observed that cell density was increased in Bioreactor Rotating & Perfusion (R&P) and Positive (Pos) control compared to Bioreactor Perfusion (P). This increase in cell density led to the formation of cellular sheets as it is obvious in Figure 4.

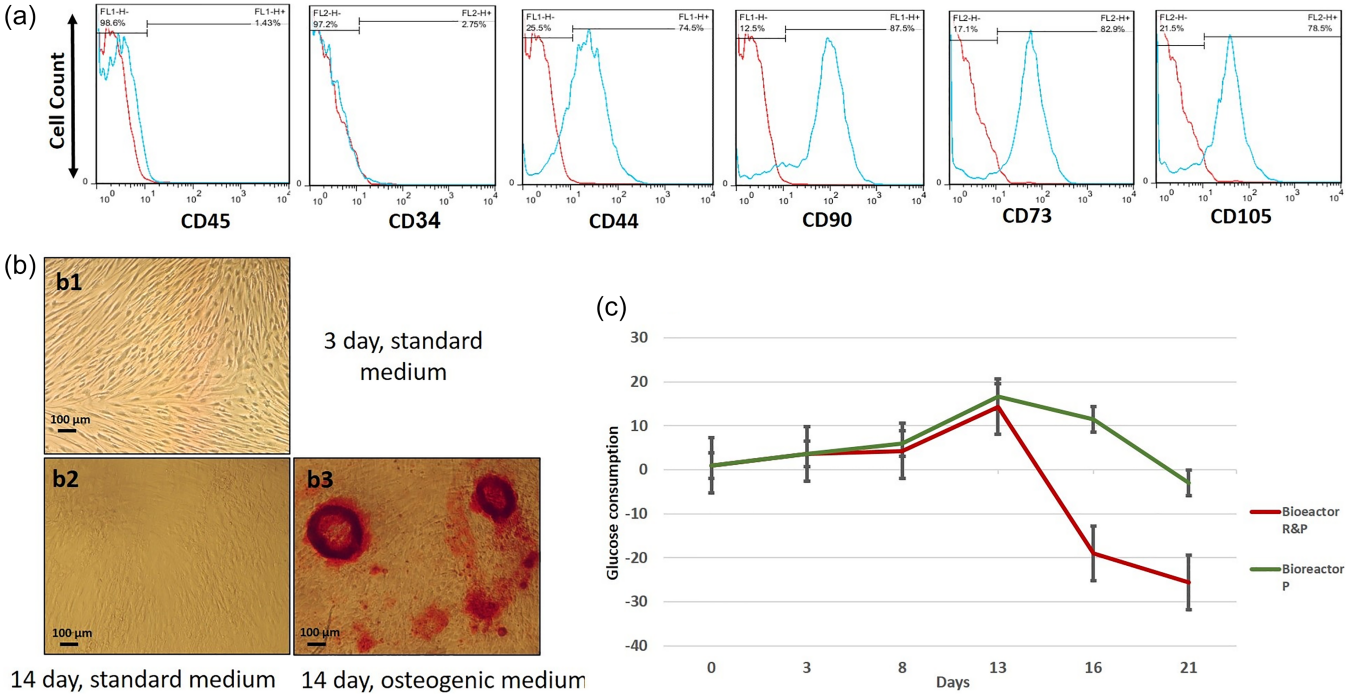

FIGURE 3 (a) Flow cytometric characterization of human buccal fat pad-derived stem cells (BFPdSCs). (b) Alizarin red staining of mesenchymal stem cells in 2D culture (b1) 3 days after cell culturing in standard and osteogenic medium. (b2, b3), respectively. (c) Rate of glucose consumption by cells, as an indicator of metabolic activity, within Bioreactor P and Bioreactor R&P. $p \leq .05$. Error bars are *SD*. ($N = 3$)

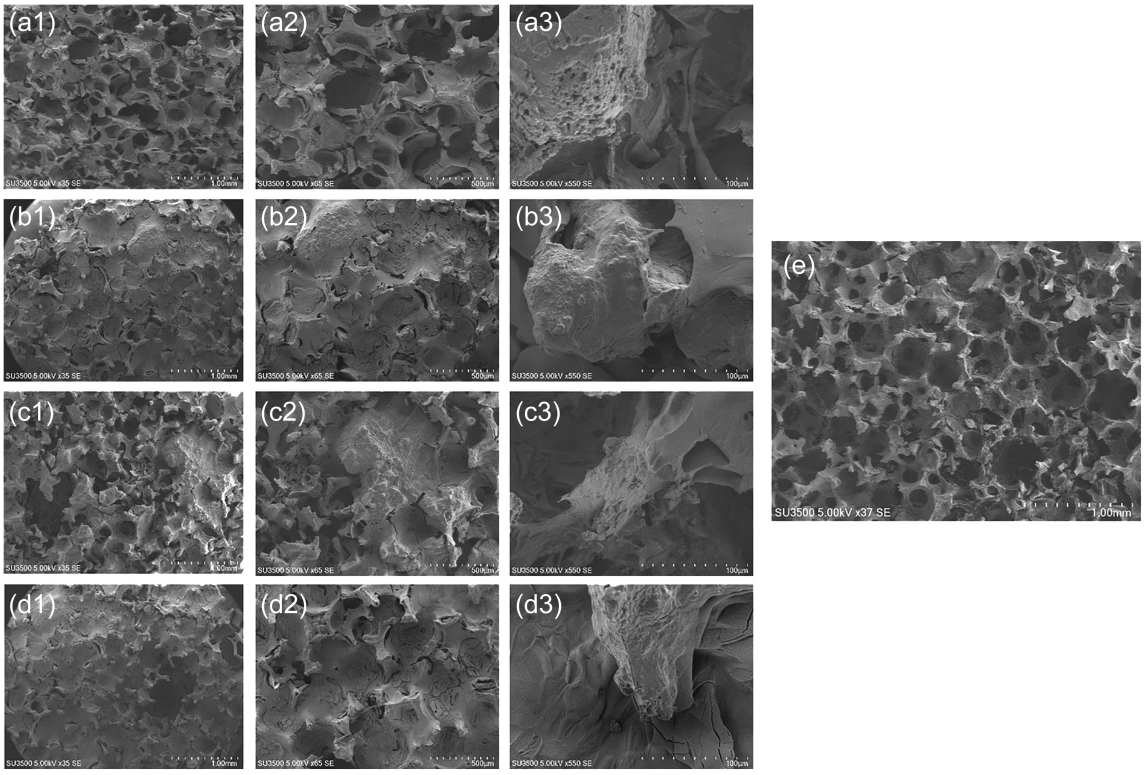

FIGURE 4 Scanning electron microscopy (SEM) observations of mesenchymal stem cells growth within the 3D gelatin coated β-tricalcium phosphate scaffolds under Neg control (a1–a3), Pos control (b1–b3), Bioreactor P (c1–c3), and Bioreactor R&P (d1–d3) after 24 days. Image (e) represents intact scaffold. SEM images of all groups show successful cell infiltration through the scaffold pores. (a3), (b3), (c3), and (d3) approve cell adhesion to the pore walls (×550 SE). (a1), (b1), (c1), (d1) (×35) and (a2), (b2), (c2), (d2) (×65) demonstrate higher cell density in Bioreactor R&P and Pos control compared to Bioreactor P in form of cellular sheet formation which filled the pore structures

3.2.3 | Histology analysis

To observe cell morphology and ECM production after exertion of dynamic force, H&E staining and Masson Trichrome staining were conducted after 24 days. A greater number of cells were observed in bioreactor specimens compared to the control groups. Moreover, in bioreactor groups, in R&P in particular, there were explicit interactions between cells and scaffolds as it demonstrated as cell sheets. (Figure 5a1,2–d1,2).

In Masson Trichrome staining, collagen fibers secreted by cells in differentiation medium were observed as blue color. Optical microscope images showed that cells secreted more collagen fibers in osteogenic medium compared to standard medium as was expected. Also, the presence of collagen fiber was prominent in Bioreactor R&P compared to Bioreactor P (Figure 5a3–d3).

3.2.4 | Osteogenic differentiation

ALP activity assay showed a significant difference between dynamic (bioreactors) and static conditions (p value ≤.05). However, comparing two bioreactors, no significant difference was observed (Figure 5e).

OCN gene was expressed significantly in Bioreactor R&P group compared to the other groups. Cells in Negative (Neg) and Pos control groups had shown similar OCN expression levels, which were significantly higher than P group. The expression of RUNX2 gene in Pos control was significantly higher than Neg control and Bioreactor P (Figure 5f).

The expression of the ALP and COL I at level of protein production was investigated qualitatively and quantitatively. The acquired data showed that Bioreactor R&P had an outstanding upregulation compared to other groups, of course, this increase is detectable in the Bioreactor P compared to static groups (Figure 6).

4 | DISCUSSION/CONCLUSION

Various designs of bioreactors are based on diversities in type, direction, and magnitude of inserted force, which influence the efficiency of bioreactors for 3D replication of lost bone. In the present study, we aimed to assess the mechanical stimulus incorporated by two types of self-designed bioreactors, that is, a rotating & perfusion and a perfusion bioreactors, on proliferation, differentiation as well as ECM

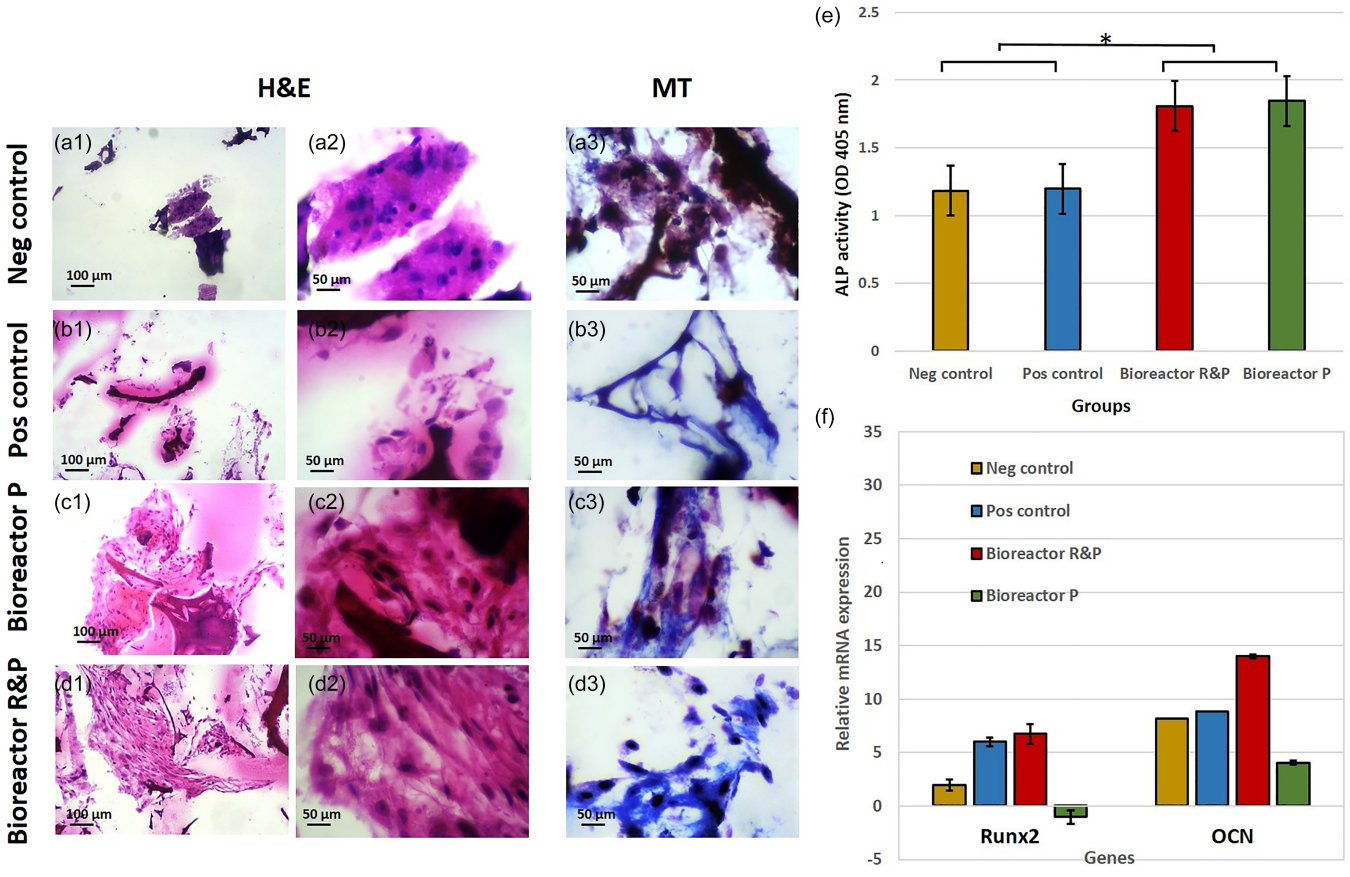

FIGURE 5 H&E staining of scaffold sections after 24 days for Neg control (a), Pos control (b), Bioreactor P (c), Bioreactor R&P (d). (a1), (b1), (c1), and (d1) are represented in 100× magnification. (a2), (b2), (c2), and (d2) are represented in 400× magnification. Masson Trichrome (MT) staining of scaffold section after 24 days for Neg control (a3), Pos control (b3), Bioreactor P (c3) and Bioreactor R&P. Images show collagen fibers in blue (400×). (e) ALP activity of cells after 24 days. Bioreactor groups showed significantly higher ALP values. (f) Relative osteogenic gene expression. Static and dynamic condition qRT-PCR for RUNX2 and OCN. β-Actin was used as an endogenous control. *p ≤ .05. (N = 3) Error bars are *SD*

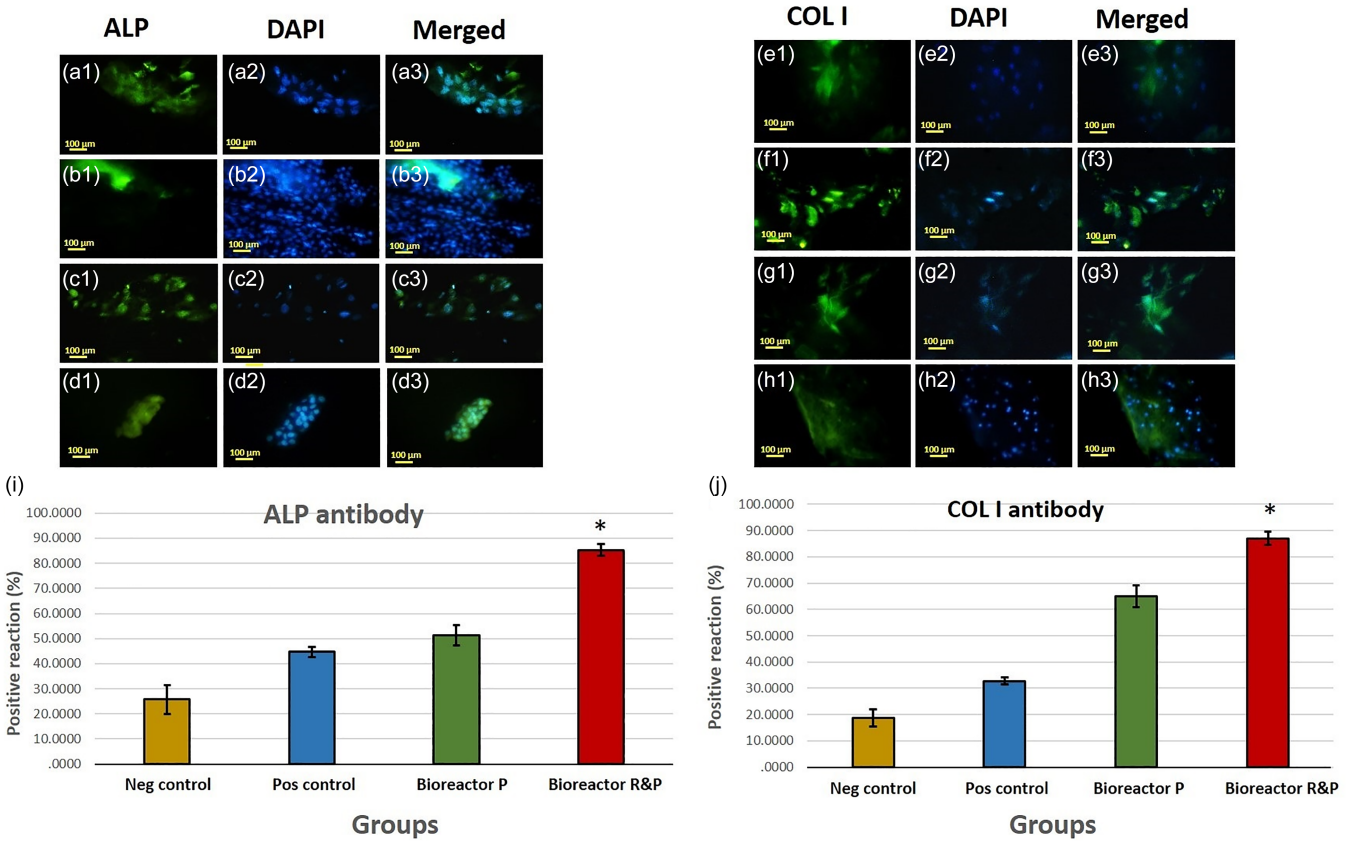

FIGURE 6 ALP Immunohistochemistry. ALP immunostaining of scaffold sections of Neg control (a1–a3), Pos control (b1–b3), Bioreactor P (c1–c3), and Bioreactor R&P (d1–d3) after 24 days. (i) Quantification of ALP antibody for groups using Image J software (e). *$p \leq .05$. ($N = 3$) Error bars are *SD*. COL I Immunohistochemistry. COL I immunostaining of scaffold sections OF Neg control (e1–e3), Pos control (f1–f3), Bioreactor P (g1–g3), and Bioreactor R&P (h1–h3) after 24 days. (j) Quantification of COL I antibody for Neg control, Pos control, Bioreactor P, and Bioreactor R&P using Image J software (e). *$p \leq .05$. ($N = 3$) Error bars are *SD*. Scale bars set to 100 µm

formation of BFPdSCs loaded on 3D scaffolds. In perfusion model, the nutrient transfer has been designed to compass the tissue-like construct in a vertically upward direction. In contrast, the perfusion of medium into the rotating & perfusion-occupied scaffolds is horizontally and constant rotation is set around the X axis. To the best of our knowledge, it is the first study to compare a novel rotating & perfusion with a previously-designed bioreactor to fabricate a large organoid bone suitable for critical-sized defects.

Majority of reports have been dedicated for comparison between dynamic and static culture condition and almost all of them have been proven the effect of bioreactor application on promotion of cellular behaviors toward the osteogenic differentiation (Du, Ushida, & Furukawa, 2015; García-Gareta, Hua, Rayan, & Blunn, 2014; Gardel, Correia-Gomes, Serra, Gomes, & Reis, 2013; Temple, Yeager, Bhumiratana, Vunjak-Novakovic, & Grayson, 2013; Wu et al., 2015). Having known that bioreactors have definite effects on cell differentiation, the next step would be to figure out the optimum force types by entering either multi-stimuli or a uni-stimulation. Jagodzinski et al. (2008) analyzed osteogenic commitment of bone marrow MSCs under cyclic mechanical and/or perfusion stimuli for a period of 21 days. They found out that exposure of scaffolds to combined mechanical stimulus enhanced cell differentiation evaluated OCN by ELIZA analysis, while the proliferation rate did not show significant differences among the groups (Jagodzinski et al., 2008). Similarly, in a study by Bölgen et al. (2008), cultured osteoblast-like cells were cultured on hydroxyethyl methacrylate-lactate-dextran in bioreactors at different regimes of perfusion and compression/perfusion. Reports of their study illustrated that activity of ALP enzyme was slightly higher in the combined type, albeit not significantly. However few researches have been conducted on the comparison of perfusion stimulation and combined forces, related papers revealed that application of a compression/perfusion bioreactor shows negligible superiority or even no differences (Bölgen et al., 2008; Liu et al., 2012). Hence, consideration of an alternative combination such as rotation plus perfusion could lead to better differentiation potential.

Our attained data covered the predominant functionality of combined bioreactor at both gene and protein levels. RUNX2 and OCN, osteogenic marker genes, was significantly higher in Bioreactor R&P. In addition, presence of great amount of ALP and COLI in Histology and IHC analysis confirmed fine gene evaluation outcomes. Although, there has been no investigation upon testing a uniaxial rotating & perfusion bioreactor, assessment of a commercial biaxial rotating & perfusion bioreactors is consistent with our results. It was demonstrated that not only these biaxial combined bioreactors do not cause any

negative changes on relative mRNA expression levels of indicators for stemness and differentiation (Leferink, Chng, van Blitterswijk, & Moroni, 2015), but also they offer a desirable environment for osteogenic induction, ALP expression, calcium deposition, and bone formation in vitro and in vivo (Zhang et al., 2009).

Dynamics of fluid principles states that direction of medium velocity is underpowered by the applied resultant forces. This rule has impressed our data, since the rotating & perfusion bioreactor with the medium flow perpendicular to the gravity force support greater cell differentiation in comparison with perfusion bioreactor that pose contradirectory fluid movement upon the earth gravitation. In the second bioreactor, the presence of converse forces on the medium could cause an invisible perturbation of the fluid and modify the proposed advantageous shear stress on the cells. Compensating the eliminated shear stress is applicable by increasing the flow rate of peristaltic pump that potentiate detachment of seeded cells. Rotating & perfusion bioreactor was designed to have a fluid flow parallel to the wall of horizontally-located chamber and the negative aspects of gravity are not as destroying as what is seen in perfusion bioreactor. This fact might be of reasons for higher cell support. On the other hand, the rotating motion of the internal axis brings a homogenous shear stress to the cells housed in the similar radius distance of the scaffolds.

The third crucial factor in determining the bioreactor effect on osteogenesis is the magnitude of fluid flow rate. In the human body, the amount of flow rate has been reported to be around 18 ml/min (Jacobs et al., 1998), while the in vitro inspections represented vast controversies in this term and delineation of an ideal range of flow rate is still a matter for debate. Nguyen, Ko, and Fisher (2016) fabricated a perfusion bioreactor and adjusted a flow rate of 20 ml/min for infusion to the femur-like scaffold. After 18 days, they found that seeded hBMSCs encapsulated in alginate indicated high viability and signs of stem cell differentiation through improved expression of ALP and BMP-2 genes and proteins. In contrary to Nguyen study, approximately all other applications of bioreactors were conducted under extremely lower flow rates. A study performed by Bancroft et al. (2002) on a perfusion bioreactor displayed that increasing the flow rate from 0.3 to 1 ml/min and 1 to 3 ml/min resulted in approximately six- and two-fold higher calcium deposition, respectively. But, protein assessment showed that after 16 days of cultivation, the scaffolds under flow rates of 0.3 ml/min secreted considerably greater amount of OCN. On the other hand, further increment of flow rates has adverse effects on cell responses as it reported in a study by Sinlapabodin, Amornsudthiwat, Damrongsakkul, and Kanokpanont (2016). They revealed that among flow rates of 1, 3, 5 ml/min, the highest flow magnitude terminated in most number of separated cells into the medium. Moreover, in spite of nearly similar number of stuck cells under flow rates of 1, 3 ml/min, post 28 days of cultivation, the latter gave the greatest osteogenic differentiation, as recognized from the significantly highest amount of ALP activity and calcium deposition. Similarly, McCoy et al. (2013), in 2012 expressed that cell incoherence is proportional to flow rate when employed flow rates of 0.05, 1, 5 ml/min. In line of the above evidences, other investigation on the flow rates of 1, 2 ml/min asserted almost equal mineralization for both (Wang, Bracaglia, Thompson, & Fisher, 2016) Conclusions, whether the exact flow rate is not yet ascertained, make clear that a range of 1–3 ml/min seems to be appealing for bone forming acceleration. In the present study, considering the fluctuation of medium delivery, we exerted the flow rate of 1–2 ml/min, which is in line with the argued papers and our prior systematic review on the bone bioreactors (Nokhbatolfoghahaei et al., 2017). However, this amount is far fewer than the measured flow rate in the neighboring of lacunar space (18 ml/min), adjustment of this scant flow appears to be logical due to the absence of ECM for cell anchorage in vitro. Given the detrimental influence of high flow rates, Sellgren and Ma (2012) revealed that they could solely reach a cell seeding efficiency of about 20% when human MSCs were cultured under the flow rate of 30 ml/min.

Our results supported the outcomes reported by other researchers that exertion of mechanical forces using multi-stimulus bioreactors is thoroughly beneficial. However, the influence of chemical condition of culturing environment such as percentage of oxygen was overlooked due requirement of specific sensors, software, and devices for precise control. Oxygen saturation is of great importance in vitro since cells of various tissue responses diversely to the amount of ambience O_2 (Weyand et al., 2015). In spite of desirable consequences of IHC assessments and gene upregulation in Bioreactor R&P, activity of ALP was not significantly above the perfusion group. In addition, H&E staining displayed no distinguishable lacuna. The absence of bone spaces and presence of cells with various differentiation stages confirmed that the study duration was not admissible for in vitro bone formation and probably elongation of cultivation period is more resultful for practical osteogenesis. Furthermore, efficiency of implanted bone constructs acquired from the bioreactors in vivo should be determined before clinical applications.

The overall outcomes of this study demonstrated that rotating & perfusion bioreactor action on bone regeneration is much preferable than perfusion bioreactor. BFPdSCs seeded on β-TCP scaffold in combined bioreactor represented higher amount of ALP activity, OCN and RUNX2 gene upregulation, and greater COLI, ALP antibodies. Therefore, it seems that exertion of multi-stimuli is more affective for bone engineering.

ACKNOWLEDGMENT

This work is supported by Iran Ministry of Health and Medical Education (Grant No. 700/1702).

CONFLICT OF INTEREST

The authors declare no potential conflict of interest.

REFERENCES

Bancroft, G. N., Sikavitsas, V. I., Van Den Dolder, J., Sheffield, T. L., Ambrose, C. G., Jansen, J. A., & Mikos, A. G. (2002). Fluid flow increases mineralized matrix deposition in 3D perfusion culture of marrow stromal osteoblasts in a dose-dependent manner. *Proceedings of the National Academy of Sciences*, *99*(20), 12600–12605.

Bastami, F., Paknejad, Z., Jafari, M., Salehi, M., Rad, M. R., & Khojasteh, A. (2017). Fabrication of a three-dimensional β-tricalcium-phosphate/gelatin containing chitosan-based nanoparticles for sustained release of bone

morphogenetic protein-2: Implication for bone tissue engineering. *Materials Science and Engineering: C*, *72*, 481–491.

Bölgen, N., Yang, Y., Korkusuz, P., Güzel, E., El Haj, A. J., & Pişkin, E. (2008). Three-dimensional ingrowth of bone cells within biodegradable cryogel scaffolds in bioreactors at different regimes. *Tissue Engineering Part A*, *14*(10), 1743–1750.

Charoenpanich, A., Wall, M. E., Tucker, C. J., Andrews, D. M., Lalush, D. S., & Loboa, E. G. (2011). Microarray analysis of human adipose-derived stem cells in three-dimensional collagen culture: Osteogenesis inhibits bone morphogenic protein and Wnt signaling pathways, and cyclic tensile strain causes upregulation of proinflammatory cytokine regulators and angiogenic factors. *Tissue Engineering Part A*, *17*(21–22), 2615–2627.

David, B., Bonnefont-Rousselot, D., Oudina, K., Degat, M.-C., Deschepper, M., Viateau, V., … Petite, H. (2011). A perfusion bioreactor for engineering bone constructs: An in vitro and in vivo study. *Tissue Engineering Part C Methods*, *17*(5), 505–516.

Du, D., Ushida, T., & Furukawa, K. S. (2015). Influence of cassette design on three-dimensional perfusion culture of artificial bone. *Journal of Biomedical Materials Research Part B Applied Biomaterials*, *103*(1), 84–91.

García-Gareta, E., Hua, J., Rayan, F., & Blunn, G. W. (2014). Stem cell engineered bone with calcium-phosphate coated porous titanium scaffold or silicon hydroxyapatite granules for revision total joint arthroplasty. *Journal of Materials Science Materials in Medicine*, *25*(6), 1553–1562.

Gardel, L. S., Correia-Gomes, C., Serra, L. A., Gomes, M. E., & Reis, R. L. (2013). A novel bidirectional continuous perfusion bioreactor for the culture of large-sized bone tissue-engineered constructs. *Journal of Biomedical Materials Research Part B Applied Biomaterials*, *101*(8), 1377–1386.

Grayson, W. L., Bhumiratana, S., Cannizzaro, C., Chao, P.-H. G., Lennon, D. P., Caplan, A. I., & Vunjak-Novakovic, G. (2008). Effects of initial seeding density and fluid perfusion rate on formation of tissue-engineered bone. *Tissue Engineering Part A*, *14*(11), 1809–1820.

Ho, A. M., Marker, P. C., Peng, H., Quintero, A. J., Kingsley, D. M., & Huard, J. (2008). Dominant negative Bmp5 mutation reveals key role of BMPs in skeletal response to mechanical stimulation. *BMC Developmental Biology*, *8*(1), 35.

Holguin, N., Brodt, M. D., & Silva, M. J. (2016). Activation of Wnt signaling by mechanical loading is impaired in the bone of old mice. *Journal of Bone and Mineral Research*, *31*(12), 2215–2226.

Hou, W. W., Zhu, Z. L., Zhou, Y., Zhang, C. X., & Yu, H. Y. (2011). Involvement of Wnt activation in the micromechanical vibration-enhanced osteogenic response of osteoblasts. *Journal of Orthopaedic Science*, *16*(5), 598–605.

Ikegame, M., Tabuchi, Y., Furusawa, Y., Kawai, M., Hattori, A., Kondo, T., & Yamamoto, T. (2016). Tensile stress stimulates the expression of osteogenic cytokines/growth factors and matricellular proteins in the mouse cranial suture at the site of osteoblast differentiation. *Biomedical Research*, *37*(2), 117–126.

Jacobs, C., Yellowley, C., Davis, B., Zhou, Z., Cimbala, J., & Donahue, H. (1998). Differential effect of steady versus oscillating flow on bone cells. *Journal of Biomechanics*, *31*(11), 969–976.

Jagodzinski, M., Breitbart, A., Wehmeier, M., Hesse, E., Haasper, C., Krettek, C., … Hankemeier, S. (2008). Influence of perfusion and cyclic compression on proliferation and differentiation of bone marrow stromal cells in 3-dimensional culture. *Journal of Biomechanics*, *41*(9), 1885–1891.

Katayama, A., Arano, T., Sato, T., Ikada, Y., & Yoshinari, M. (2012). Radial-flow bioreactor enables uniform proliferation of human mesenchymal stem cells throughout a three-dimensional scaffold. *Tissue Engineering Part C Methods*, *19*(2), 109–116.

Leferink, A. M., Chng, Y.-C., van Blitterswijk, C. A., & Moroni, L. (2015). Distribution and viability of fetal and adult human bone marrow stromal cells in a biaxial rotating vessel bioreactor after seeding on polymeric 3D additive manufactured scaffolds. *Frontiers in Bioengineering and Biotechnology*, *3*, 169.

Li, M., Wu, W., Tan, L., Mu, D., Zhu, D., Wang, J., & Zhao, B. (2015). Low-magnitude mechanical vibration regulates expression of osteogenic proteins in ovariectomized rats. *Biochemical and Biophysical Research Communications*, *465*(3), 344–348.

Lim, K.-T., Kim, J., Seonwoo, H., Chang, J. U., Choi, H., Hexiu, J., … Chung, J. H. (2012). Enhanced osteogenesis of human alveolar bone-derived mesenchymal stem cells for tooth tissue engineering using fluid shear stress in a rocking culture method. *Tissue Engineering Part C Methods*, *19*(2), 128–145.

Liu, C., Abedian, R., Meister, R., Haasper, C., Hurschler, C., Krettek, C., … Jagodzinski, M. (2012). Influence of perfusion and compression on the proliferation and differentiation of bone mesenchymal stromal cells seeded on polyurethane scaffolds. *Biomaterials*, *33*(4), 1052–1064.

Liu, L., Zong, C., Li, B., Shen, D., Tang, Z., Chen, J., … Wang, J. (2014). The interaction between β1 integrins and ERK1/2 in osteogenic differentiation of human mesenchymal stem cells under fluid shear stress modelled by a perfusion system. *Journal of Tissue Engineering and Regenerative Medicine*, *8*(2), 85–96.

McCoy, R. J., & O'Brien, F. J. (2010). Influence of shear stress in perfusion bioreactor cultures for the development of three-dimensional bone tissue constructs: A review. *Tissue Engineering Part B Reviews*, *16*(6), 587–601.

McCoy, R. J., Widaa, A., Watters, K. M., Wuerstle, M., Stallings, R. L., Duffy, G. P., & O'Brien, F. J. (2013). Orchestrating osteogenic differentiation of mesenchymal stem cells—Identification of placental growth factor as a mechanosensitive gene with a pro-osteogenic role. *Journal of Stem Cells*, *31*(11), 2420–2431.

Nguyen, B. N. B., Ko, H., & Fisher, J. P. (2016). Tunable osteogenic differentiation of hMPCs in tubular perfusion system bioreactor. *Biotechnology and Bioengineering*, *113*(8), 1805–1813.

Nokhbatolfoghahaei, H., Rad, M. R., Khani, M.-M., Nadjmi, N., & Khojasteh, A. (2017). Application of bioreactors to improve functionality of bone tissue engineering constructs: A systematic review. *Current Stem Cell Research & Therapy*, *12*(7), 564–599.

Qian, X., Yuan, F., Zhimin, Z., & Anchun, M. (2013). Dynamic perfusion bioreactor system for 3D culture of rat bone marrow mesenchymal stem cells on nanohydroxyapatite/polyamide 66 scaffold in vitro. *Journal of Biomedical Materials Research Part B: Applied Biomaterials*, *101*(6), 893–901.

Rauh, J., Milan, F., Guenther, K.-P., & Stiehler, M. (2011). Bioreactor systems for bone tissue engineering. *Tissue Engineering Part B Reviews*, *17*(4), 263–280.

Rezai Rad, M., Bohloli, M., Akhavan Rahnama, M., Anbarlou, A., Nazeman, P., & Khojasteh, A. (2017). Impact of tissue harvesting sites on the cellular behaviors of adipose-derived stem cells: Implication for bone tissue engineering. *Stem Cells International*, *2017*, 1–9.

Salehi-Nik, N., Rezai Rad, M., Kheiri, L., Nazeman, P., Nadjmi, N., & Khojasteh, A. (2017). Buccal fat pad as a potential source of stem cells for bone regeneration: A literature review. *Stem Cells International*, *2017*, 1–13.

Sellgren, K. L., & Ma, T. (2012). Perfusion conditioning of hydroxyapatite–chitosan–gelatin scaffolds for bone tissue regeneration from human mesenchymal stem cells. *Journal of Tissue Engineering and Regenerative Medicine*, *6*(1), 49–59.

Sinlapabodin, S., Amornsudthiwat, P., Damrongsakkul, S., & Kanokpanont, S. (2016). An axial distribution of seeding, proliferation, and osteogenic differentiation of MC3T3-E1 cells and rat bone marrow-derived mesenchymal stem cells across a 3D Thai silk fibroin/gelatin/hydroxyapatite scaffold in a perfusion bioreactor. *Materials Science and Engineering Part C*, *58*, 960–970.

Temple, J. P., Yeager, K., Bhumiratana, S., Vunjak-Novakovic, G., & Grayson, W. L. (2013). Bioreactor cultivation of anatomically shaped human bone

grafts. In G. Vunjak-Novakovic & K. Turksen (Eds.), *Biomimetics and Stem Cells* (pp. 57–78). New York, NY: Humana Press.

Vetsch, J. R., Müller, R., & Hofmann, S. (2015). The evolution of simulation techniques for dynamic bone tissue engineering in bioreactors. *Journal of Tissue Engineering and Regenerative Medicine*, *9*(8), 903–917.

Wang, H., Wang, R., Wang, Z., Liu, Q., Mao, Y., & Duan, X. (2015). ClC-3 chloride channel functions as a mechanically sensitive channel in osteoblasts. *Biochemistry and Cell Biology*, *93*(6), 558–565.

Wang, M. O., Bracaglia, L., Thompson, J. A., & Fisher, J. P. (2016). Hydroxyapatite-doped alginate beads as scaffolds for the osteoblastic differentiation of mesenchymal stem cells. *Journal of Biomedical Materials Research Part A*, *104*(9), 2325–2333.

Weyand, B., Nöhre, M., Schmälzlin, E., Stolz, M., Israelowitz, M., Gille, C., … Vogt, P. M. (2015). Noninvasive oxygen monitoring in three-dimensional tissue cultures under static and dynamic culture conditions. *BioResearch Open Access*, *4*(1), 266–277.

Wu, W., Le, A. V., Mendez, J. J., Chang, J., Niklason, L. E., & Steinbacher, D. M. (2015). Osteogenic performance of donor-matched human adipose and bone marrow mesenchymal cells under dynamic culture. *Tissue Engineering Part A*, *21*(9–10), 1621–1632.

Wu, Y., Zhang, X., Zhang, P., Fang, B., & Jiang, L. (2012). Intermittent traction stretch promotes the osteoblastic differentiation of bone mesenchymal stem cells by the ERK1/2-activated Cbfa1 pathway. *Connective Tissue Research*, *53*(6), 451–459.

Yeatts, A. B., Both, S. K., Yang, W., Alghamdi, H. S., Yang, F., Fisher, J. P., & Jansen, J. A. (2013). In vivo bone regeneration using tubular perfusion system bioreactor cultured nanofibrous scaffolds. *Tissue Engineering Part A*, *20*(1–2), 139–146.

Zhang, P., Wu, Y., Jiang, Z., Jiang, L., & Fang, B. (2012). Osteogenic response of mesenchymal stem cells to continuous mechanical strain is dependent on ERK1/2-Runx2 signaling. *International Journal of Molecular Medicine*, *29*(6), 1083–1089.

Zhang, Z.-Y., Teoh, S. H., Chong, W.-S., Foo, T.-T., Chng, Y.-C., Choolani, M., & Chan, J. (2009). A biaxial rotating bioreactor for the culture of fetal mesenchymal stem cells for bone tissue engineering. *Biomaterials*, *30*(14), 2694–2704.

SUPPORTING INFORMATION

Additional supporting information may be found online in the Supporting Information section at the end of this article.

How to cite this article: Nokhbatolfoghahaei H, Bohlouli M, Paknejad Z, et al. Bioreactor cultivation condition for engineered bone tissue: Effect of various bioreactor designs on extra cellular matrix synthesis. *J Biomed Mater Res*. 2020; 108:1662–1672. https://doi.org/10.1002/jbm.a.36932